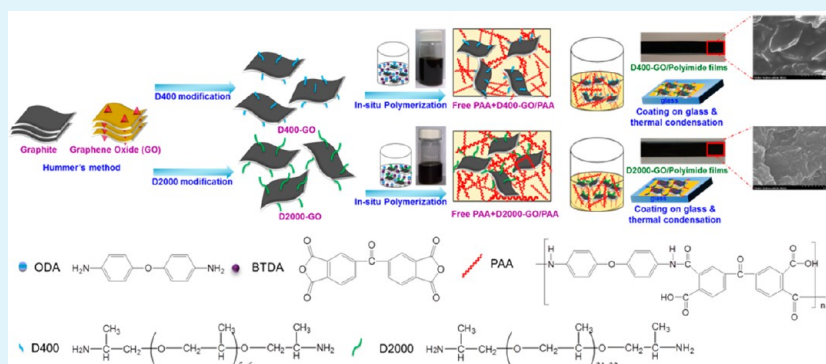


Effect of Molecular Chain Length on the Mechanical and Thermal Properties of Amine-Functionalized Graphene Oxide/Polyimide Composite Films Prepared by In Situ Polymerization

Wei-Hao Liao, Shin-Yi Yang, Jen-Yu Wang, Hsi-Wen Tien, Sheng-Tsung Hsiao, Yu-Sheng Wang, Shin-Ming Li, Chen-Chi M. Ma,* and Yi-Fang Wu

Department of Chemical Engineering, National Tsing-Hua University, Hsin-Chu 30013, Taiwan, R.O.C.

Supporting Information



ABSTRACT: This study fabricates amine (NH_2)-functionalized graphene oxide (GO)/polyimide (PI) composite films with high performance using in situ polymerization. Linear poly(oxyalkylene)amines with two different molecular weights 400 and 2000 (D400 and D2000) have been grafted onto the GO surfaces, forming two types of NH_2 -functionalized GO (D400-GO/D2000-GO). NH_2 -functionalized GO, especially D400-GO, demonstrated better reinforcing efficiency in mechanical and thermal properties. The observed property enhancement are due to large aspect ratio of GO sheets, the uniform dispersion of the GO within the PI matrix, and strong interfacial adhesion due to the chemical bonding between GO and the polymeric matrix. The Young's modulus of the composite films with 0.3 wt % D400-GO loading is 7.4 times greater than that of neat PI, and tensile strength is 240% higher than that of neat PI. Compared to neat PI, 0.3 wt % D400-GO/PI film exhibits approximately 23.96 °C increase in glass transition temperature (T_g). The coefficient of thermal expansion below T_g is significantly decreased from 102.6 $\mu\text{m}/^\circ\text{C}$ (neat PI) to 53.81 $\mu\text{m}/^\circ\text{C}$ (decreasing 48%) for the D400-GO/PI composites with low D400-GO content (0.1 wt %). This work not only provides a method to develop the GO-based polyimide composites with superior performances but also conceptually provides a chance to modulate the interfacial interaction between GO and the polymer through designing the chain length of grafting molecules on NH_2 -functionalized GO.

KEYWORDS: graphene oxide, amine-functionalized, polyimide, composites, in situ polymerization

INTRODUCTION

Polymer composites with carbon-based nanofillers have generated significant interest in industry and science, since they have multifunctional and valuable properties and do not sacrifice the processability and add excessive weight. Carbon-based nanofillers, particularly carbon nanotubes (CNTs), have the potential to reinforce various polymer types in various applications, such as thermal management, electronics, and energy applications.^{1–6} These potential applications arise from the unique nanostructures and excellent physical properties of CNTs that are based on the building block of all graphitic allotropes: graphene. However, unresolved and critical issues limit their practical applications, such as (1) poor dispersion of CNTs in the polymeric matrix; (2) limited availability of high-quality nanotubes; and (3) the high cost of CNT.^{1,4,7–9}

Graphene-based nanomaterials have recently provided an alternative method of fabricating multifunctional composites because of their superior properties and the natural abundance of their base material, graphite. Graphene-based materials, such as graphene nanosheets (GNSs) and graphene oxide (GO), show great potential for improving the properties of polymer composites. This is due to their extraordinarily high surface area, high conductivity, unique graphitized planar structure, and low manufacturing costs.^{1,7–12}

GO differs greatly from GNSs regarding chemical structure, leading to the wider potential for further functionalization. GO

Received: October 29, 2012

Accepted: January 2, 2013

Published: January 2, 2013

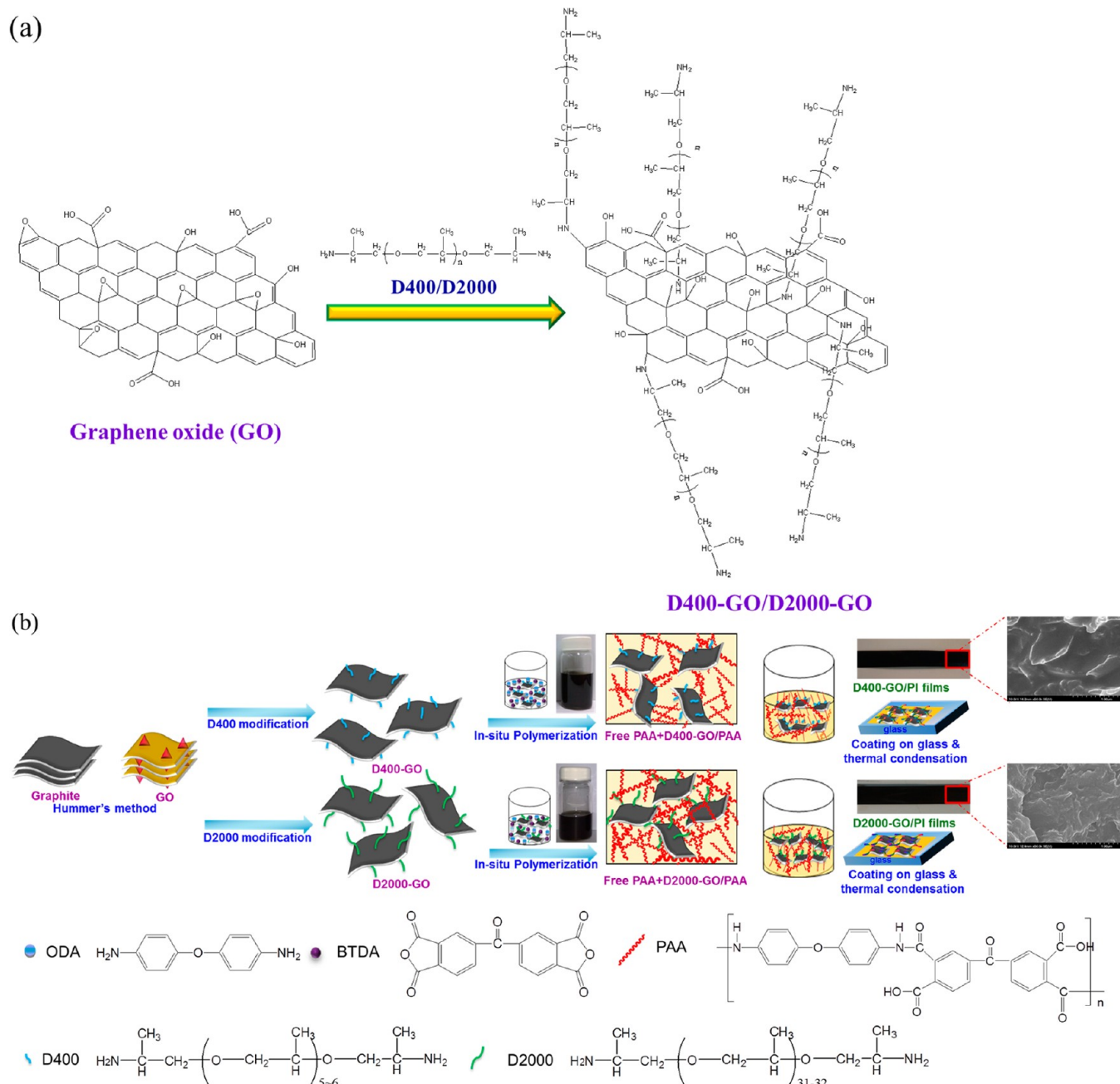


Figure 1. (a) Reaction schematics between GO and poly (oxyalkylene)amine. (b) Scheme of the procedure for preparation of D400-GO/PI and D2000-GO/PI films.

consists of a two-dimensional sheet of covalently bonded carbon atoms bearing various oxygen functional groups (e.g., hydroxyl, epoxide, and carbonyl groups) on the basal planes and edges.^{6,13–15} These oxygen functional groups on the GO surface provide versatile sites for chemical functionalization, imparting improved compatibility and reinforcing efficiency of GO in polymeric matrixes. Therefore, it is valuable to design and synthesize the properties of GO-filled polymer composites using various functionalizing approaches to modulate the interphase structure between GO and the polymer host. Despite previous reports on the improved polymer properties following the incorporation of GO, the actual performances of GO-filled polymer composites are lower than the anticipated values, which were estimated from the ultrahigh surface area and superior mechanical properties of GO. The reinforcing

efficiency between GO and polymer was reduced, because GO sheets restacked and aggregated^{4,16–23}

Therefore, it is a critical issue to resolve these problems to optimize the GO efficiency for reinforcing nanofillers to polymeric hosts. In our previous research,²⁴ we have reported that the in situ polymerization is an effective approach to fabricate GO/PI (polyimide) composite films because NH_2 -functionalized GO acts as a starting platform for grafting polymer.

This study further designed NH_2 -functionalized GO/PI composite films to approach uniform dispersion of NH_2 -functionalized GO in the PI matrix and to construct flexible, hierarchical, and covalently bonded interphase structures between NH_2 -functionalized GO and PI. The NH_2 -functionalized GO decorated with molecular weight of 400 and 2000

poly(oxyalkylene)amines (D400 and D2000) not only prohibited the restacking of the GO sheets to achieve excellent dispersion but also acted as a versatile starting platform for the in situ fabrication of composite films by grafting poly(amic acid) (PAA, the precursor of polyimide) at the GO-reactive sites. Compared with the neat PI film, the D400-GO/PI film exhibited a dramatic improvement in mechanical and thermal properties at low GO loadings, indicating that the GO, combined with long molecular chains and amine functional group, is important for the in situ preparation of PI-based composite films with large surface area and outstanding properties.

EXPERIMENTAL SECTION

Materials. Poly(propylene glycol) bis(2-aminopropyl ether) with average molecular weights of ~ 400 (D400) and ~ 2000 (D2000) was purchased from Aldrich Chemical Co. 3,3',4,4'-Benzophenonetetracarboxylic dianhydride (BTDA) was also obtained from Aldrich Chemical Co. Nano Graphites (NGPs) were supplied by Angstrom Materials LLC, McCook Avenue, Dayton, Ohio, USA, which were produced by a chemical vapor deposition (CVD) process. The thickness of the NGPs was smaller than 100 nm. Potassium permanganate (KMnO_4), sodium nitrate (NaNO_3), dimethylacetamide (DMAc), and sulfuric acid (H_2SO_4) were received from the Showa Chemical Co., Tokyo, Japan.

Preparation of GO. In 1957, Hummers and Offeman developed a safe, quick, and efficient process to prepare GO.¹⁵ On the basis of Hummers method, H_2SO_4 (50 mL) was poured into a 250 mL three-neck flask and stirred in an ice bath, and the temperature was maintained at about 0 °C. NGPs (2 g) and NaNO_3 (1 g) were added and stirred uniformly. KMnO_4 (30 g) was added slowly to the mixture in the reaction vessel with an ice bath over 30 min. The solution was heated to 35 °C, and the oxidation was allowed to proceed for 24 h. Then, distilled water was added slowly, and the temperature was controlled below 100 °C. This reaction was terminated by adding a large amount of distilled water and 30% H_2O_2 solution (6 mL). The mixture was filtered and washed with distilled water. This process was repeated several times until the pH of the percolate reached 7. The sample of GO was obtained after drying in a vacuum oven.

Preparation of D400-GO/PI and D2000-GO/PI Films through In Situ Polymerization Process. GO (54.8 mg, containing about 30% epoxide group) was dispersed in anhydrous DMAc, (20 mL) using tip sonication (1 h) leading to dispersed GO sheets in solution homogeneously. D400 (0.164 g, 0.41 mmol)/D2000 was charged into a 100 mL three-necked flask equipped with a magnetic stirrer and nitrogen inlet and outlet, and the reaction mixture was refluxed and stirred at 60 °C for 24 h under a nitrogen atmosphere. Functionalization of GO with D400/D2000 was assigned as D400-GO/D2000-GO. Then, BTDA (3.2 g, 0.01 mol) and oxydianiline (ODA, 2g, 0.01 mol) were charged. The mixture was stirred at room temperature for 24 h and then poured into a glass dish, followed by vacuum evaporation at 30 °C for 48 h and heat-treatment at 100, 150, 200, and 300 °C for 2 h and then at 400 °C for 5 min. The film thickness is about 0.1 mm. The D400-GO/PI and D2000-GO/PI composite films containing 0.1, 0.3, and 1.0 wt % of D400-GO/D2000-GO were prepared by the above-mentioned experimental steps. Figure 1a shows the reaction schematics between GO and poly(oxyalkylene)amine; Figure 1b shows the procedure for preparing D400-GO/PI and D2000-GO/PI films.

Characterization and Instruments. The scanning electron microscope (SEM) used in this work was a Hitachi S-4200 SEM (Hitachi Limited, Tokyo, Japan) with an accelerating voltage of 15 kV. Fourier transfer infrared spectroscopy (FT-IR) spectra of samples were recorded between 400 and 4000 cm^{-1} on a Nicolet Avatar 320 FT-IR spectrometer, Nicolet Instrument Corporation, Madison, WI, USA. The sample was coated on a CaF_2 plate. An Ultima IV multipurpose X-ray diffraction (XRD) system (Rigaku Co., Sendagaya, Shibuya-Ku, Tokyo, Japan) was used for the X-ray analysis with $\text{Cu K}\alpha$

radiation ($\lambda = 1.54051 \text{ \AA}$). Step scanning was used with 2θ intervals from 5° to 80° with a residence time of 1 s. Transmission electron microscope (TEM) observations were conducted using a JEM-2100 microscope (JEOL Limited, Tokyo, Japan) with 200 kV. Thermogravimetric (TGA) analyses were performed with a Du Pont TGA 2900 analyzer from 30 to 800 °C in nitrogen (N_2) at a heating rate of 10 °C min^{-1} . To measure the tensile strength and modulus of the PI films, samples were cut to sheets with a width of 10 mm and were tested using an Universal Testing Machine (Tinius Olsen H10K-S Benchtop Testing Machine). The test procedure followed ASTM-D882. Dimensions of test specimen were 50 mm \times 5 mm \times 0.1 mm; the crosshead speed was 5 mm min^{-1} . Thermal expansion of composites was characterized by a thermo mechanical analyzer (Universal TA Instruments 2940 TMA V2.4E) at a ramp rate of 10 °C/min.

RESULTS AND DISCUSSION

Morphology of GO, D400-GO, and D2000-GO. Figure 2 shows the TEM morphology of the GO, D400-GO, and D2000-GO. GO shows a smooth carpet-like structure (Figure 2a). Compared to GO, poly(oxyalkylene)amines-grafted GO exhibited a rougher and encapsulating structure (Figure 2b,c), suggesting the successful grafting of poly(oxyalkylene)amines on GO through nucleophilic attack by amine on the epoxy groups. The long molecular chains of poly(oxyalkylene)amines were easily entangled and coiled up during the solvent evaporation procedure, further forming encapsulating and globular morphology on the GO surface. GO, D400-GO, and D2000-GO all possessed unique 2D nanostructures that were different from the structures of carbon black or graphite. Therefore, the GO-based materials exhibited large aspect ratios that enhanced the contact areas with the polymeric matrix. This was an important factor in the improvement of the GO-filled polymer composite performance.

Characterizations of GO, D400-GO, and D2000-GO. To further characterize the structures of GO, D400-GO, and D2000-GO, XRD was employed to observe their graphitic (002) faces (Figure 3). The XRD pattern of GO showed a sharp diffraction peak at approximately 11°, corresponding to an interlayer spacing of 0.78 nm.^{25,26} The interlayer spacing indicates a larger spacing between GO layers. This larger space could be attributed to wrinkling or presence of functional groups in the interlayer structure. Following modification with poly(oxyalkylene)amines, the (002) diffraction peaks of D400-GO and D2000-GO significantly shifted to a smaller angle region (5° and 3°, respectively) and weakened intensity compared to that of GO, revealing that the poly(oxyalkylene)amines (D400/D2000) were inserted in the GO sheets to further increase the interlayer distances and structural heterogeneity. Furthermore, the presence of long molecular chains on the GO surface can restrain the restacking of the planar GO nanosheet, inducing ordered graphitic stacking to well-disorder structures.

FT-IR is a technique which is used to obtain an accurate band and chemistry of the surface modifiers. To demonstrate the actual occurrence of chemical reactions between poly(oxyalkylene) amines and GO, FT-IR spectrum of different samples were recorded (as shown in Figure 4). The characteristic features related to GO were observed at 3475 cm^{-1} (O–H stretching), 2973 and 2891 cm^{-1} (C–H stretching), 1623 cm^{-1} (C=O stretching), 1522 cm^{-1} (O–H bending), 1094 cm^{-1} (C–O stretching), and 1020 cm^{-1} (C–O–C stretching).^{27,28} After GO reacted with poly(oxyalkylene) amines, the FT-IR spectra of both D400-GO and D2000-GO exhibited the additional peaks of N–H stretching at 3455 and

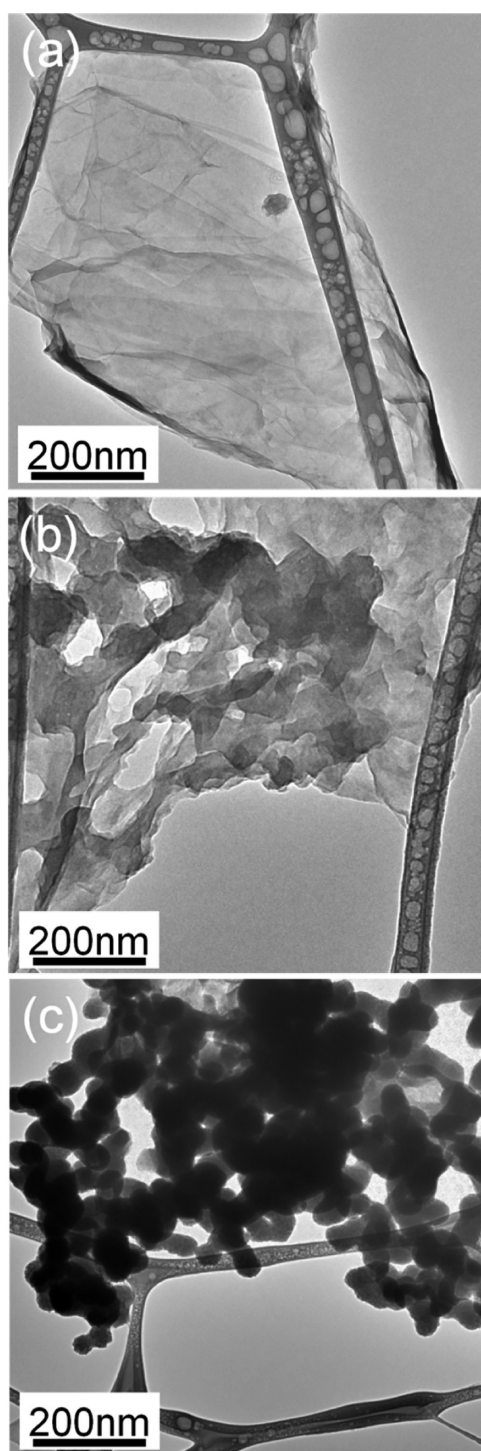


Figure 2. TEM images of (a)GO, (b)D400-GO, and (c)D2000-GO.

3409 cm^{-1} and the C–N stretching peak at 1226 cm^{-1} .^{29,30} The result of FT-IR indicates that a ring-opening reaction did occur between the amine groups of poly(oxyalkylene) amines and the epoxy groups on GO surface,³¹ forming C–N covalent bonding, demonstrating that the poly(oxyalkylene) amines were grafted onto GO sheets successfully. The presence of C–N bonds is in agreement with the expected structures of poly(oxyalkylene)amines-grafted GO, as shown in Figure 1. Consequently, TEM, XRD, and FT-IR results confirmed that poly(oxyalkylene) amines were grafted on the GO sheets successfully.

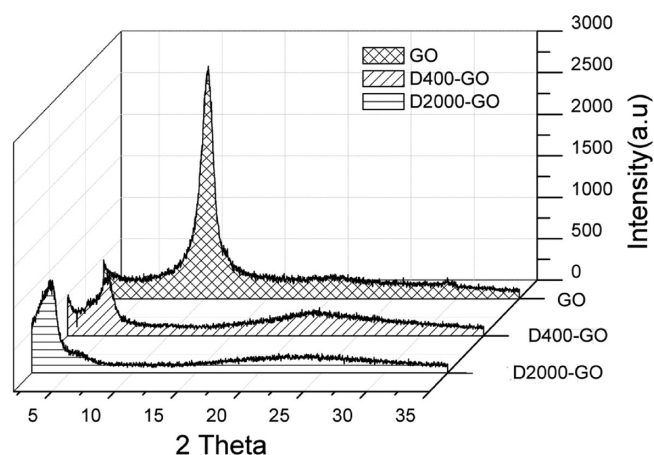


Figure 3. X-ray diffraction patterns of GO, D400-GO, and D2000-GO.

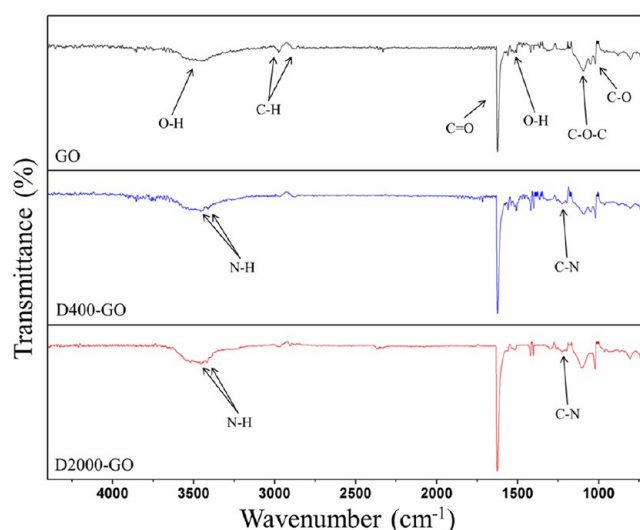


Figure 4. FT-IR spectrum of GO, D400-GO, and D2000-GO.

TGA is a useful tool to characterize the quantity of the organic substances grafted on GO. Covalent bonds generally form between the graphene sheet, and its substituents are thermally stripped in the temperature range of $200\text{--}500\text{ }^{\circ}\text{C}$.³²

Figure 5 shows typical TGA thermograms indicating the weight loss of material. For as-prepared GO, a significant weight loss can be found above $200\text{ }^{\circ}\text{C}$, which was caused by the decomposition of oxygen-containing functional groups. Because GO sheets bear oxygen-containing functional groups with strong hydrophilic properties, water molecules are bound tightly into their stacked structure.²² Compared to the thermal decomposition behavior of GO, the poly(oxyalkylene)amine-grafted GO sheets exhibited significantly different weight loss curves and thermally degraded in two stages. In the first stage, between 200 and $300\text{ }^{\circ}\text{C}$, slight weight loss was caused by the thermal degradation of the unreacted oxygen-containing functional group. The significant weight loss that occurred in the second stage (300 to $450\text{ }^{\circ}\text{C}$) was caused by the degradation of the poly(oxyalkylene)amines attached to the surface of D400-GO and D2000-GO. Furthermore, the quantity of surface-grafted poly(oxyalkylene)amines on GO sheets was estimated by comparing the weight loss of GO in the region between 300 and $450\text{ }^{\circ}\text{C}$. TGA results indicated that the weight fraction of organic substances of D400-GO and

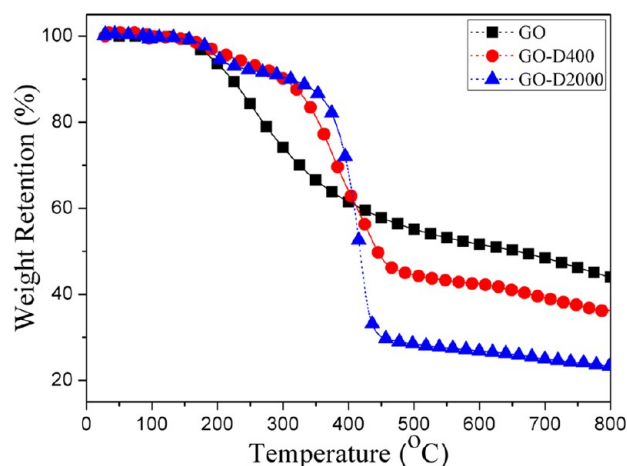


Figure 5. TGA curves of GO, D400-GO, and D2000-GO (heating rate of 10 °C/min, in nitrogen).

D2000-GO can be estimated as approximately 18.1 wt % and approximately 13.9 wt %, respectively. The poly(oxyalkylene)-amines substituted epoxide groups to further alter the surface properties of GO, reducing the weight loss at low temperatures. In summary, analyzing the results from XRD, FT-IR, and TGA clearly show that the graphene oxide sheets were successfully functionalized by reaction with the poly(oxyalkylene)amines. The rest of this study provides an effective method of achieving well-dispersed GO, and poly(oxyalkylene)amine-grafted GO can disperse well in organic solvents, allowing in situ polymerization. The premodified poly(oxyalkylene)amine-grafted GO provides a versatile platform for fabricating polymer composite materials by grafting of polymer.

Morphology of D400-GO/PI and D2000-GO/PI Films.

High-resolution SEM images of the fractured surfaces of the sample (as shown in Figure 6) were used to investigate the dispersion and compatibility of D400-GO and D2000-GO in a PI matrix following tensile testing. Figure 6a,b shows a smooth surface of the neat PI, exhibiting the unidirectional stripes of

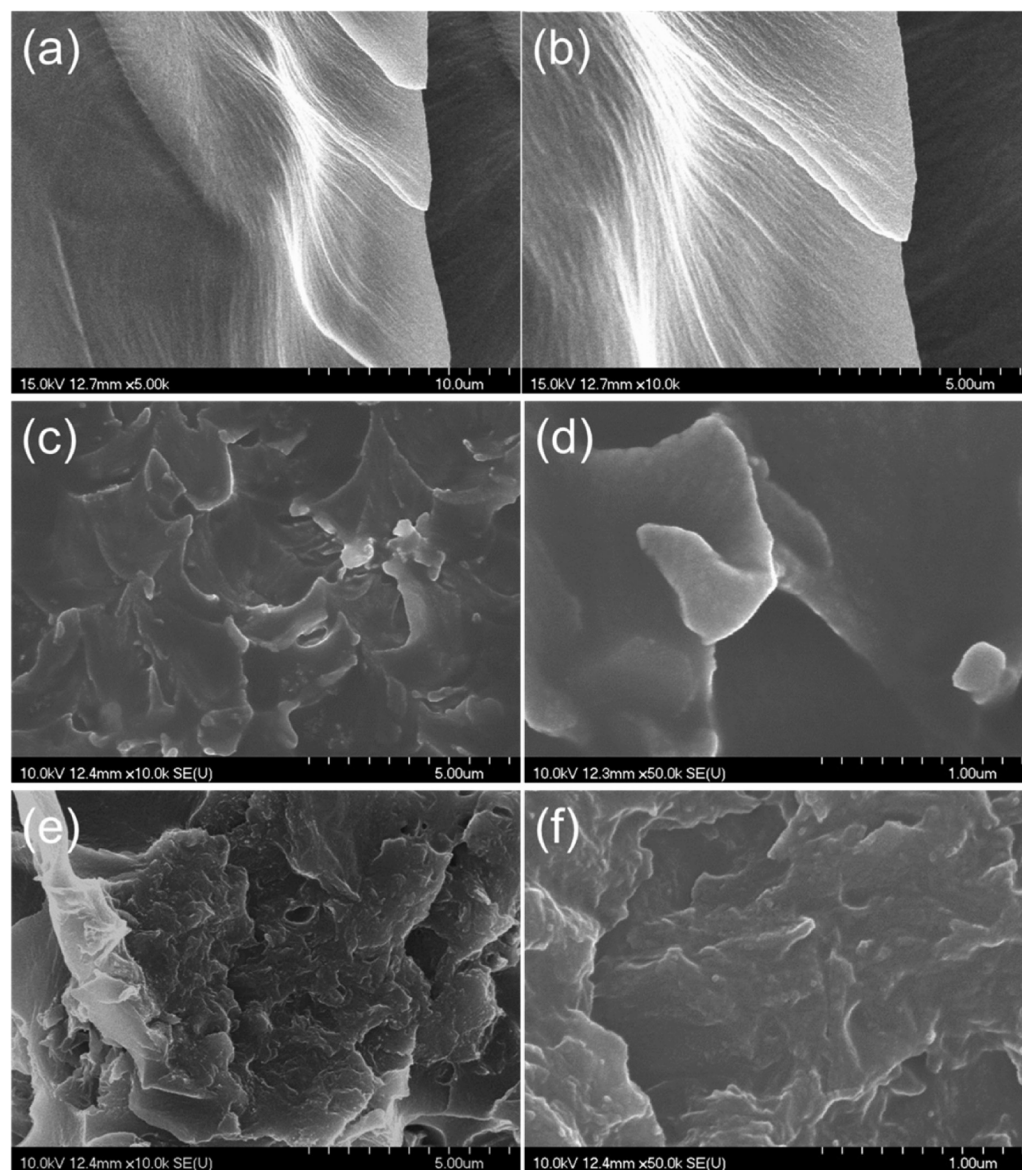


Figure 6. SEM images of fractured surface of (a) neat PI films ($\times 5k$), (b) neat PI films ($\times 10k$), (c) 0.3 wt % D400-GO/PI films ($\times 10k$), (d) 0.3 wt % D400-GO/PI films ($\times 50k$), (e) 0.3 wt % D2000-GO/PI films ($\times 10k$), and (f) 0.3 wt % D2000-GO/PI films ($\times 50k$).

Table 1. Mechanical Properties of Neat PI Film, D400-GO/PI Films, and D2000-GO/PI Films

sample	tensile modulus/GPa	tensile strength/MPa	elongation at break (%)
neat PI films	1.92 ± 0.08	80.1 ± 5.8	6.61 ± 0.31
0.1 wt % D400-GO/PI films	5.07 ± 0.26	129.0 ± 9.3	2.57 ± 0.52
0.3 wt % D400-GO/PI films	16.12 ± 0.68	270.1 ± 15.6	1.75 ± 0.13
1.0 wt % D400-GO/PI films	14.15 ± 0.53	198.0 ± 13.2	0.92 ± 0.08
0.1 wt % D2000-GO/PI films	4.68 ± 0.23	95.0 ± 6.9	0.66 ± 0.05
0.3 wt % D2000-GO/PI films	12.82 ± 0.58	122.2 ± 8.7	0.88 ± 0.07
1.0 wt % D2000-GO/PI films	10.76 ± 0.51	102.2 ± 8.0	0.58 ± 0.04

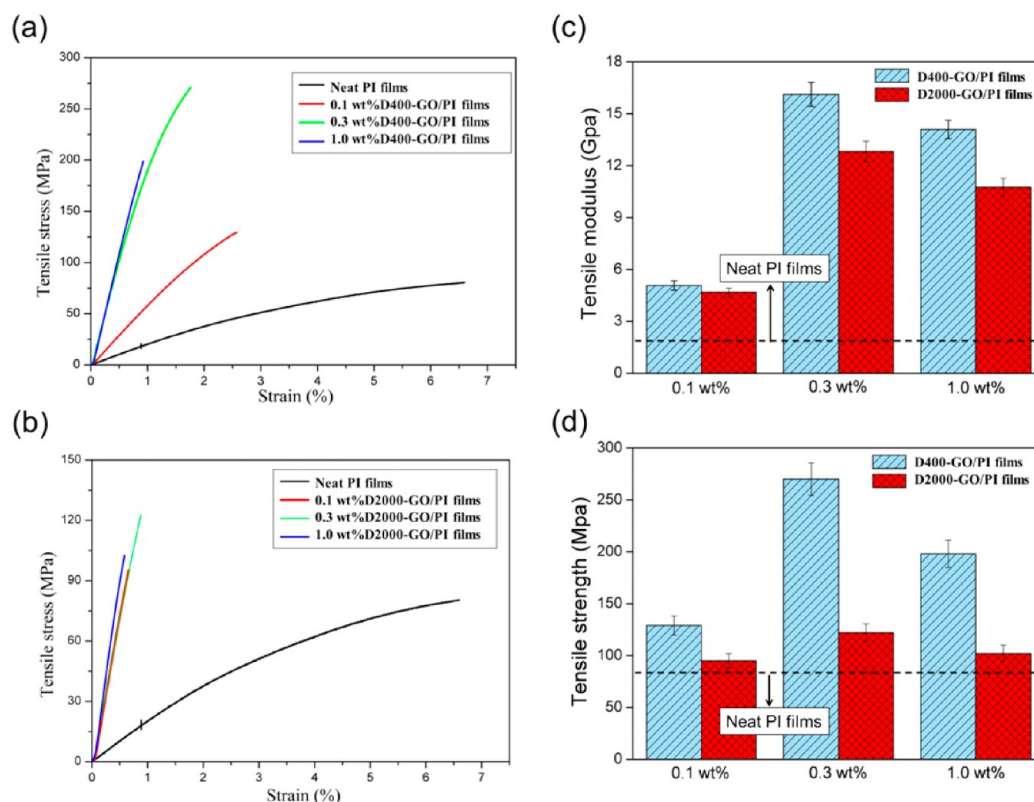


Figure 7. (a) Stress–strain curves of neat PI films and D400-GO/PI films with various amounts of D400-GO. (b) Stress–strain curves of neat PI films and D2000-GO/PI films with various D2000-GO content. (c) Tensile modulus and (d) tensile strength of neat PI film, D400-GO/PI films, and D2000-GO/PI films.

bearing load. For the SEM image of D400-GO, almost no agglomerates were formed, implying that D400-GO shows the variation of roughness on the fractured surface of D400-GO/PI films. Furthermore, D400-GO was tightly embedded in the films, suggesting the excellent compatibility and homogeneity of D400-GO/PI films. Consequently, the amine-rich surface of D400-GO provided a starting platform for polymer grafting. The high grafting density was used to construct a flexible interface that achieved homogeneous dispersion of graphene nanosheets in composite films and strengthened the interfacial interaction with the polymer matrix.²⁴ Compared with D400-GO/PI film, the SEM image of D2000-GO/PI film showed heterogeneity, the formation of defects, and higher roughness on the fractured surface. This phenomenon revealed that the introduction of long molecular chains on the GO surface results in low compatibility between GO and the PI matrix. Although the long molecular chain on D2000-GO should effectively prohibit the restacking of GO, the steric hindrance resulting from the entangled molecular chains reduces the reactivity of amine-functional groups to form the poly(amic acid)-D2000-

GO completely. Therefore, the proper molecular chain length on GO with amine-functional groups favors the formation of strong and flexible interfaces between GO and the PI matrix, increasing the polymer-reinforcing efficiency of GO.

Mechanical Properties of D400-GO/PI and D2000-GO/PI Films. To investigate the reinforcing effect of D400-GO and D2000-GO in composite films, the tensile modulus and tensile strengths of composite films at various GO loadings (0.1, 0.3, and 1 wt %) were compared. In this study, 10 samples for each film were tested to analyze the data. The tensile modulus, tensile strength, and elongation at the break are summarized in Table 1 and Figure 7. As the D400-GO loading increased from 0 to 0.3 wt %, the tensile modulus and tensile strength increased from 1.92 GPa and 80 MPa to 16.12 GPa and 270 MPa, respectively. Compared to neat PI films, the D400-GO/PI film with only 0.3 wt % D400-GO exhibited a dramatic increase in tensile modulus (approximately 7.4 times) and a significant improvement in tensile strength (approximately 240%) as well, revealing that D400-GO had a superior efficiency for promoting the load transfer between the polymer

and D400-GO. This superior efficiency may be caused by the excellent dispersion of D400-GO in the polymeric matrix, as well as the formation of strong flexible interfaces between GO and the PI matrix, which may have benefited from the long molecular chains and amine functionality on the D400-GO surface.

However, the tensile modulus and tensile strength of the D2000-GO/PI films containing 0.1 wt % D2000-GO was increased to 4.68 GPa and 95 MPa, respectively. When the D2000-GO content was increased from 0.1 to 0.3 wt %, the tensile modulus increased from 4.68 to 12.82 GPa (approximately 5.7 times increase over neat PI film), and a tensile strength of 122 MPa (approximately 52% increase over neat PI film) was achieved. Compared to D400, D2000 possesses more flexible chain rigidity, which plays the role of transferring load from PI matrix to GO. However, the reinforcing efficiency of D2000-GO was significantly lower than that of D400-GO, which was consistent with the SEM observations (Figure 6e,f). Consequently, two reasons are proposed for the limited improvements in tensile properties of the composite films: (1) steric hindrance resulting from the long and entangled molecular chains reduced the reactivity of the amine-functional groups to form the poly(amic acid)-D2000-GO completely, decreasing the interfacial interaction to restrict the movement of the polymer chain and (2) the covalent-linkage between D2000-GO and the PI polymer segment was too long to efficiently promote the load transfer. In addition, as the GO content increased further from 0.3 to 1.0 wt %, the reinforcing efficiency of both D400-GO and D2000-GO decreased slightly, and a similar trend was also found for the tensile modulus of composite material. When the filler reached a critical content, the distance between any two sheets was so small that the van der Waals forces became significant and the sheets were agglomerated, consequently, reducing the aspect ratio of GO, and the reinforcing efficiency was reduced. Therefore, an appropriate filled-content of GO can optimize the contribution to mechanical properties.

In summary, these two types of NH_2 -functionalized GO with differing lengths of linear molecular chains showed superior tensile properties, suggesting that these NH_2 -functionalized GO act as a versatile starting platform for the in situ polymerization of composite films to acquire the benefits of the large aspect ratios of GO sheets, the excellent dispersion of GO within the PI matrix, and strong interfacial adhesion caused by the chemical bonding between GO and the polymeric matrix. In addition, designing the length of molecular chain on GO can optimize their reinforcing efficiency for the mechanical strength of composite film. Furthermore, the strategy of polymer grafting modulated a flexible and hierarchical interphase between the polymer and the graphene oxide sheet to provide an effective method for load transfer.

Thermal Properties of D400-GO/PI and D2000-GO/PI Film. The coefficients of thermal expansions (CTE) and glass transition temperature (T_g) of the neat PI, D400-GO/PI, and D2000-GO/PI composite films were analyzed by TMA, showing the interfacial interaction between the PI matrix and the graphene (Figure 8 and Table 2). On the basis of previous studies,^{33,34} incorporating pure GO into a polymer matrix through solution blending generally decreases the thermal properties because the presence of aggregated GO causes increases in viscosity and steric hindrance, influencing the cross-linking density of the composite. The low cross-linking density of the composite causes an increase in the mobility of the

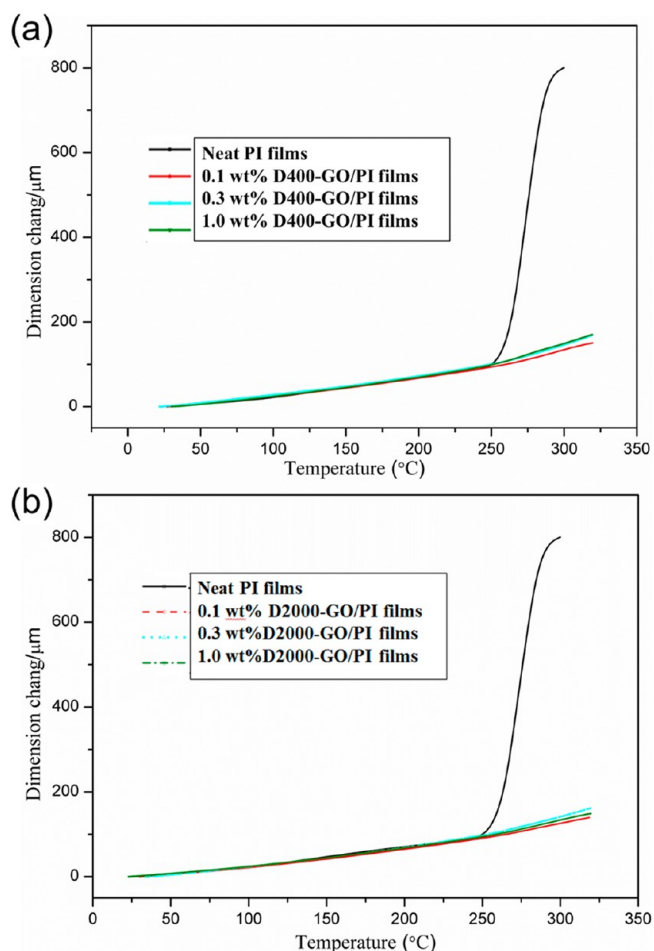


Figure 8. TMA curves of (a) neat PI film and D400-GO/PI films and (b) neat PI film and D2000-GO/PI films.

polymer segments. However, T_g of the D400-GO/PI films containing only 0.3 wt % D400-GO (approximately 297.45 °C) was much higher than that of neat PI film (273.49 °C). Furthermore, CTE of D400-GO/PI films containing only 0.3 wt % D400-GO also demonstrated a significant decrease compared to neat PI film, demonstrating that incorporating D400-GO into the PI matrix restricts the mobility of the polymer chains significantly. T_g and CTE of D2000-GO/PI films showed significant improvements, compared with neat PI film. However, the reinforcing efficiency of D2000-GO was significantly lower than that of D400-GO, which was consistent with the results of SEM and the tensile properties.

There are two reasons proposed for the remarkable improvements to the tensile and thermal properties of these composite films: First, the NH_2 -functionalized GO decorated with molecular weight 400 and 2000 poly(oxyalkylene)amines (D400-GO and D2000-GO) maintained excellent dispersion of the GO within the PI matrix during in situ polymerization, further forming a 3D network throughout the entire polymer matrix and maximizing the contact area between GO and the PI polymer. Second, the amine-rich surface of GO provided a starting platform for grafting polymer, and the high grafting density constructed flexible, hierarchical, and covalently bonded interphase structures between NH_2 -functionalized GO and PI to achieve a strong interfacial interaction and to restrain the movement of the polymer segments.²⁴ Furthermore, this study provided a chance to modulate the interfacial interaction

Table 2. Thermal Properties of Neat PI Film, D400-GO/PI Films, and D2000-GO/PI Films

sample	T_g (°C)	CTE below T_g ($\mu\text{m}/^\circ\text{C}$)	CTE above T_g ($\mu\text{m}/^\circ\text{C}$)
neat PI films	273.5 ± 2.1	102.6 ± 1.8	343.2 ± 2.3
0.1 wt % D400-GO/PI films	294.6 ± 1.7	53.8 ± 1.2	93.4 ± 1.3
0.3 wt % D400-GO/PI films	297.5 ± 1.1	62.6 ± 1.4	147.5 ± 1.8
1.0 wt % D400-GO/PI films	293.5 ± 1.4	56.9 ± 0.9	130.2 ± 1.9
0.1 wt % D2000-GO/PI films	280.2 ± 0.9	55.9 ± 0.6	74.5 ± 0.8
0.3 wt % D2000-GO/PI films	295.7 ± 0.8	61.7 ± 0.9	134.5 ± 1.7
1.0 wt % D2000-GO/PI films	292.4 ± 1.6	58.0 ± 0.8	86.7 ± 0.9

between GO and the polymer by modifying the chain length of the grafting molecules on NH_2 -functionalized GO.

CONCLUSION

In this study, two linear poly(oxyalkylene)amines with differed molecular weights were grafted onto the GO surface successfully, forming two types of NH_2 -functionalized GO (D400-GO and D2000-GO). These NH_2 -functionalized GO can act as versatile starting platforms for in situ polymerization to obtain lightweight, strong, GO-based polyimide composite materials with superior performances. On the basis of the results of SEM and TMA, as well as the tensile properties, proper molecular chain length on GO with amine-functional groups will enhance the polymer reinforcing efficiency of GO because of the large aspect ratio GO sheets, the well-dispersed GO in the PI matrix, and the strong interfacial adhesion resulting from the covalent bonding between GO and the polymeric matrix. The D400-GO/PI films with 0.3 wt % D400-GO loading exhibited an approximate 7.4 times increase in tensile modulus and a 240% improvement in tensile strength compared to neat PI. In addition, the CTE below T_g was significantly decreased from 102.6 $\mu\text{m}/^\circ\text{C}$ (neat PI film) to 53.81 $\mu\text{m}/^\circ\text{C}$ for the D400-GO/PI composite films with a low D400-GO content (0.1 wt %). Furthermore, this study not only provides a method for developing GO-based polyimide composite materials with superior performances but also conceptually provides a chance to modulate the interfacial interaction between GO and polymer by designing the chain length of grafting molecules on NH_2 -functionalized GO.

ASSOCIATED CONTENT

Supporting Information

The surface morphologies, obtained using atomic force microscopy (AFM), showing the AFM 2D and 3D images of GO, D400-GO, and D2000-GO. The SEM images of neat PI and GO/PI composites with the poly(oxyalkylene) amines modified GO content from 0.1 to 1.0 wt %. The TGA curves of D400 and D2000 materials exhibiting the temperature range of thermal degradation. A high resolution X-ray photoelectron spectrometer elucidating the surface composition of GO, D400-GO, and D2000-GO. This information is available free of charge via the Internet at <http://pubs.acs.org/>.

AUTHOR INFORMATION

Corresponding Author

*Tel: 886-35713058. Fax: 886-35715408. E-mail: ccma@che.nthu.edu.tw.

Notes

The authors declare no competing financial interest.

ACKNOWLEDGMENTS

This work was supported by the National Science Council, Taipei, Taiwan, Republic of China, under contract no. NSC-101-2221-E-007-031, and the boost program from the Low Carbon Energy Research Center in National Tsing Hua University.

REFERENCES

- Rafiee, M. A.; Rafiee, J.; Wang, Z.; Song, H.; Yu, Z.-Z.; Koratkar, N. *ACS Nano* **2009**, *3*, 3884–3890.
- Coleman, J. N.; Khan, U.; Blau, W. J.; Gun'ko, Y. K. *Carbon* **2006**, *44*, 1624–1652.
- Zhang, Z.; Zhang, J.; Chen, P.; Zhang, B.; He, J.; Hu, G.-H. *Carbon* **2006**, *44*, 692–698.
- Mitchell, C. A.; Bahr, J. L.; Arepalli, S.; Tour, J. M.; Krishnamoorti, R. *Macromolecules* **2002**, *35*, 8825–8830.
- Calvert, P. *Nature* **1999**, *399*, 210.
- Wang, H.; Hao, Q.; Yang, X.; Lu, L.; Wang, X. *ACS Appl. Mater. Interfaces* **2010**, *2*, 821–828.
- Li, D.; Kaner, R. B. *Science* **2008**, *320*, 1170–1171.
- Stankovich, S.; Dikin, D. A.; Dommett, G. H.; Kohlhaas, K. M.; Zimney, E. J.; Stach, E. A.; Piner, R. D.; Nguyen, S. T.; Ruoff, R. S. *Nature* **2006**, *442*, 282–286.
- Kim, H.; Abdala, A. A.; Macosko, C. W. *Macromolecules* **2010**, *43*, 6515–6530.
- Verdejo, R.; Bernal, M. M.; Romasanta, L. J.; Lopez-Manchado, M. A. *J. Mater. Chem.* **2011**, *21*, 3301–3310.
- Cai, D.; Song, M. *J. Mater. Chem.* **2010**, *20*, 7906–7915.
- Lee, C.; Wei, X.; Kysar, J. W.; Hone, J. *Science* **2008**, *321*, 385–388.
- Huang, T.; Lu, R. G.; Su, C.; Wang, H. N.; Guo, Z.; Liu, P.; Huang, Z. Y.; Chen, H. M.; Li, T. S. *ACS Appl. Mater. Interfaces* **2012**, *4*, 2699–2708.
- Hontoria-Lucas, C.; López-Peinado, A. J.; López-González, J. d. D.; Rojas-Cervantes, M. L.; Martín-Aranda, R. M. *Carbon* **1995**, *33*, 1585–1592.
- Hummers, W. S.; Offeman, R. E. *J. Am. Chem. Soc.* **1958**, *80*, 1339–1339.
- Chen, D.; Zhu, H.; Liu, T. *ACS Appl. Mater. Interfaces* **2010**, *2*, 3702–3708.
- Chen, L.; Chai, S. G.; Liu, K.; Ning, N. Y.; Gao, J.; Liu, Q. F.; Chen, F.; Fu, Q. *ACS Appl. Mater. Interfaces* **2012**, *4*, 4398–4404.
- Hsiao, M. C.; Liao, S. H.; Yen, M. Y.; Liu, P. I.; Pu, N. W.; Wang, C. A.; Ma, C. C. M. *ACS Appl. Mater. Interfaces* **2010**, *2*, 3092–3099.
- Stankovich, S.; Piner, R. D.; Nguyen, S. T.; Ruoff, R. S. *Carbon* **2006**, *44*, 3342–3347.
- Liu, J.; Tang, J.; Gooding, J. J. *J. Mater. Chem.* **2012**, *22*, 12435–12452.
- Cui, L.; Tarte, N. H.; Woo, S. I. *Macromolecules* **2008**, *41*, 4268–4274.
- Xu, Z.; Gao, C. *Macromolecules* **2010**, *43*, 6716–6723.
- Luong, N. D.; Hipp, U.; Korhonen, J. T.; Soininen, A. J.; Ruokolainen, J.; Johansson, L.-S.; Nam, J.-D.; Sinh, L. H.; Seppälä, J. *Polymer* **2011**, *52*, 5237–5242.

- (24) Wang, J.-Y.; Yang, S.-Y.; Huang, Y.-L.; Tien, H.-W.; Chin, W.-K.; Ma, C.-C. *M. J. Mater. Chem.* **2011**, *21*, 13569–13575.
- (25) Yang, S.-Y.; Chang, K.-H.; Tien, H.-W.; Lee, Y.-F.; Li, S.-M.; Wang, Y.-S.; Wang, J.-Y.; Ma, C.-C. M.; Hu, C.-C. *J. Mater. Chem.* **2011**, *21*, 2374–2380.
- (26) Lv, W.; Tang, D.-M.; He, Y.-B.; You, C.-H.; Shi, Z.-Q.; Chen, X.-C.; Chen, C.-M.; Hou, P.-X.; Liu, C.; Yang, Q.-H. *ACS Nano* **2009**, *3*, 3730–3736.
- (27) Pham, V. H.; Cuong, T. V.; Hur, S. H.; Oh, E.; Kim, E. J.; Shin, E. W.; Chung, J. S. *J. Mater. Chem.* **2011**, *21*, 3371–3377.
- (28) Park, S.; Dikin, D. A.; Nguyen, S. T.; Ruoff, R. S. *J. Phys. Chem. C* **2009**, *113*, 15801–15804.
- (29) Shan, C.; Yang, H.; Han, D.; Zhang, Q.; Ivaska, A.; Niu, L. *Langmuir* **2009**, *25*, 12030–12033.
- (30) Xu, Y.; Liu, Z.; Zhang, X.; Wang, Y.; Tian, J.; Huang, Y.; Ma, Y.; Zhang, X.; Chen, Y. *Adv. Mater.* **2009**, *21*, 1275–1279.
- (31) Compton, O. C.; Dikin, D. A.; Putz, K. W.; Brinson, L. C.; Nguyen, S. T. *Adv. Mater.* **2010**, *22*, 892–896.
- (32) Dyke, C. A.; Tour, J. M. *Nano Lett.* **2003**, *3*, 1215–1218.
- (33) Wang, S.; Tambraparni, M.; Qiu, J.; Tipton, J.; Dean, D. *Macromolecules* **2009**, *42*, 5251–5255.
- (34) Teng, C.-C.; Ma, C.-C. M.; Lu, C.-H.; Yang, S.-Y.; Lee, S.-H.; Hsiao, M.-C.; Yen, M.-Y.; Chiou, K.-C.; Lee, T.-M. *Carbon* **2011**, *49*, 5107–5116.